Nature of doped *a*-Si:H/*c*-Si interface recombination

Stefaan De Wolf[1,a)] and Michio Kondo[2]
[1]*Ecole Polytechnique Fédérale de Lausanne (EPFL), Photovoltaics and Thin Film Electronics Laboratory, Breguet 2, CH-2000 Neuchâtel, Switzerland*
[2]*National Institute of Advanced Industrial Science and Technology (AIST), Central 2, 1-1-1 Umezono, Tsukuba, Ibaraki 305-8568, Japan*

(Received 10 December 2008; accepted 8 April 2009; published online 26 May 2009)

Doped hydrogenated amorphous silicon (*a*-Si:H) films of only a few nanometer thin find application in *a*-Si:H/crystalline silicon heterojunction solar cells. Although such films may yield a field effect at the interface, their electronic passivation properties are often found to be inferior, compared to those of their intrinsic counterparts. In this article, based on H_2 effusion experiments, the authors argue that this phenomenon is caused by Fermi energy dependent Si–H bond rupture in the *a*-Si:H films, for either type of doping. This results in the creation of Si dangling bonds, counteracting intentional doping of the *a*-Si:H matrix, and lowering the passivation quality. © *2009 American Institute of Physics*. [DOI: 10.1063/1.3129578]

I. INTRODUCTION

Semiconducting heterostructures increasingly attract attention for electronic junction formation in crystalline silicon (*c*-Si) wafer based solar cells. A key point of such a device is the displacement of highly recombination-active (Ohmic) contacts from the silicon surface by insertion of a film with wide bandgap. To reach the full device potential, the heterointerface state density should be minimal.[1] Practically, hydrogenated amorphous silicon (*a*-Si:H) films are appealing candidates for this: Their bandgap is wider than that of *c*-Si and, when intrinsic, such films can reduce the *c*-Si surface state density by hydrogenation.[2] In addition, these films can be doped relatively easily, either *n*- or *p*-type, allowing for the fabrication of electronically abrupt *p*-*n* and low-high heterojunctions (HJ).[3] Doping of these films may be expected to yield a built-in electrical field, repelling either electrons or holes from the surface states. In principle, this could suppress the *a*-Si:H/*c*-Si interface recombination further, in a similar way as, e.g., in back-surface-field homojunction solar cells.[4] Experimentally, however, such layers have been found to result sometimes in poorer electronic passivation of *c*-Si surfaces than their intrinsic counterparts.[5–7] For this reason, typically, a few nanometer thin intrinsic buffer layer is inserted between the *c*-Si surface and the doped *a*-Si:H films for device fabrication.[8] For HJ solar cells featuring such stacked film structures, impressive large area (>100 cm^2) energy conversion efficiencies (>22%) have been reported.[9,10] Despite this result, the fundamental origin of the poor passivation of the doped *a*-Si:H/*c*-Si interface is not yet fully understood.

In this article, we propose that the dependency of the electronic surface passivation on the *a*-Si:H film doping is linked to Fermi energy (E_F) dependent Si–H bond rupture in such films. The latter phenomenon is attributed to the position of E_F within the bandgap, influencing the generation of (native) compensation defects in the semiconductor, counteracting intentional doping.

II. EXPERIMENTAL

For the experiments, 320 μm thick 0.7 Ω cm phosphorus-doped high quality float zone (100) (FZ)-Si wafers were used. Both substrate surfaces were mirror polished to eliminate the influence of substrate surface roughness on the passivation properties.[11] Prior to deposition, the samples were immersed in a piranha solution (H_2SO_4:H_2O_2) (4:1) for 10 min to grow a chemical oxide, followed by rinsing in de-ionized water. The oxide was then stripped off in a dilute HF solution (5%) for 30 s. To avoid cross contamination, a clustered multichamber parallel plate plasma enhanced chemical vapor deposition (PECVD) system, consisting of separate chambers for *a*-Si:H(*i*), *a*-Si:H(n^+), and *a*-Si:H(p^+) layer deposition was used. After transfer of the samples to the relevant deposition chambers and mounting at the top electrodes, the wafer surfaces were exposed to a 200 SCCM (SCCM denotes cubic centimeter per minute at STP) H_2 flow for 20 min at a pressure of 0.5 Torr for temperature stabilization of the samples. The spacing between electrode and sample was 20 mm when depositing intrinsic films, whereas for doped layer depositions this was 22 mm. During film deposition, all chambers were operated at radio frequency (13.56 MHz) power. For soft film deposition, the used power was consistently the minimum required to maintain a stable plasma. The B_2H_6 and PH_3 concentrations were 4660 and 1550 ppm in H_2, respectively. No additional H_2 dilution was used during deposition. To avoid epitaxial growth during deposition, the intrinsic and p^+-films were deposited at 155 °C. Due to the relatively higher H_2 dilution factor for the n^+-films, their deposition temperature T_{depo} was reduced to 120 °C, for the same reason. All deposition conditions are summarized in Table I, unless otherwise stated.

To evaluate the surface passivation quality of the respective films, identical structures were deposited on both wafer

a)Electronic mail: stefaan.dewolf@epfl.ch.

TABLE I. Film deposition conditions, unless otherwise stated

Parameter	a-Si:H(i)	a-Si:H(p^+)	a-Si:H(n^+)
Power density (mW cm^{-2})	12	36	36
Electrode distance (mm)	20	22	22
[SiH_4] (SCCM)	20	10	10
[B_2H_6] (SCCM)	···	30	···
[PH_3] (SCCM)	···	···	100
Pressure (Torr)	0.5	0.5	0.5
T_{depo}(°C)	155	155	120
t_{depo} (s)	108	60	150

surfaces. For the stacked doped structures, first the intrinsic buffer layer was deposited on both sides of the samples prior to doped layer deposition, to avoid cross contamination of the interfaces. Before each intrinsic deposition, the samples were immersed in a dilute (5%) HF solution for 30 s. Post-deposition annealing offers in a straightforward way a single parameter to vary both electronic and material properties of the samples under study. For this, following deposition, the samples were consecutively subjected to stepwise isochronal annealing treatments in a vacuum furnace (20 °C increment per step of 30 min, with annealing temperatures (T_{ann}^{step}) ranging from 120 °C to 260 °C). In between these annealing steps, the value for effective carrier lifetime (τ_{eff}) of the samples was measured with a Sinton Consulting WCT-100 quasi-steady-state photoconductance (QSSPC) system,[12] operated in the so-called *generalized* mode. Unless otherwise stated, all reported values for τ_{eff} were evaluated at a constant carrier injection density, $\Delta n = \Delta p = 1.0 \times 10^{15}$ cm^{-3}. Since high quality (FZ)-Si wafers were used, the values for τ_{eff} can be considered as a measure for the surface passivation quality. The deposited film thickness (d_{bulk}) as well as other film properties were determined by measuring ellipsometry spectra (ψ,Δ) using a variable angle Woollam M-2000 rotating-compensator instrument. These data were then fitted to a two-layer (Tauc–Lorentz) model, taking the 50% void surface roughness thickness (d_{rough}) of the deposited material into account.[13] For bulk characterization of the films, thermal desorption spectroscopy (TDS) measurements were taken of 1 cm^2 samples. For this an ESCO EMD-WA1000S system operated at ultrahigh vacuum ($<1.0 \times 10^{-9}$ Torr) was used in which the samples are lamp-heated up to 1000 °C, with a linear temperature ramp of 20 K min^{-1}. During the annealing, a Balzers AG QMG 421 quadrupole mass spectrometer was used to determine the H_2 effusion rate from the a-Si:H films.

III. RESULTS

Figure 1(a) shows the change in surface passivation quality, expressed by τ_{eff}, as a function of the described stepwise annealing treatment for, respectively, a few nanometer thin intrinsic, n^+- and p^+-doped single film a-Si:H/c-Si heterostructures. Whereas annealing up to 260 °C has a beneficial effect on the surface passivation properties of a-Si:H(i) films, the same treatment is seen to result immediately in losses for the a-Si:H(p^+) case. For a-Si:H(n^+) films, initially an improvement in passivation quality can be seen. Nevertheless, annealing above 220 °C results also here in losses. Figure 1(b) shows how the optical bandgap (E_G^{opt}) of these films, extracted from spectroscopic ellipsometry (SE) measurements, changes during the annealing treatment. Interestingly, in both cases where the passivation degrades, it coincides with a collapse of E_G^{opt}. The latter phenomenon may point at defect formation in the amorphous host.

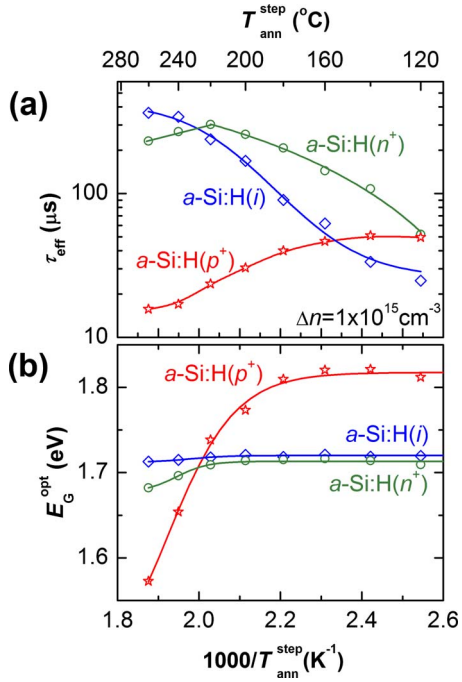

FIG. 1. (Color online) (a) Influence of stepwise annealing on the interface passivation quality of a few nanometer thin single film a-Si:H/c-Si structure, expressed by τ_{eff} (at $\Delta n = \Delta p = 1.0 \times 10^{15}$ cm^{-3}) and extracted from QSSPC measurements. No intrinsic buffer layers are present underneath the doped films. Symmetric structures have been deposited on both wafer surfaces. (b) Influence of stepwise annealing treatment on the optical bandgap E_G^{opt} of the same films as in (a), extracted from SE measurements. Symbols represent experimental data; the lines are guides for the eye.

Figure 2 shows for the a-Si:H(p^+)/c-Si case the inverse

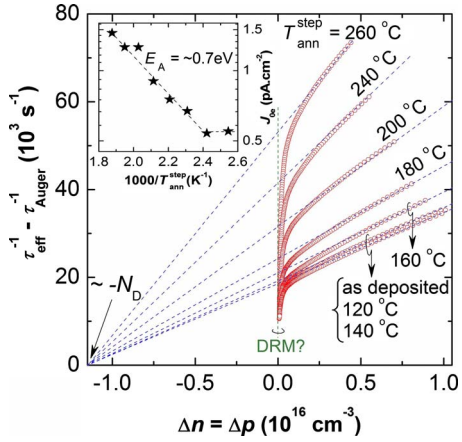

FIG. 2. (Color online) Inverse effective carrier lifetime (corrected for Auger recombination) as function of carrier injection density for an n-type FZ-Si wafer bifacially passivated by a few nanometer thin a-Si:H(p^+) films. The respective curves show data following thermal annealing at given temperatures. The dashed lines are asymptotic fits of the data to expression (1). The graph in the inset shows the extracted J_{0e} values as function of the inverse annealing temperature.

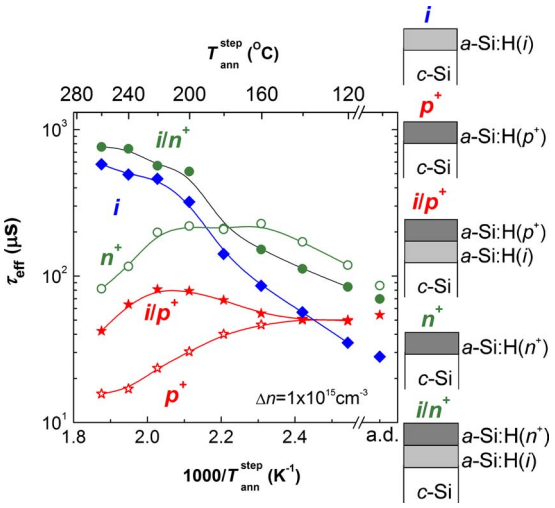

FIG. 3. (Color online) Influence of stepwise annealing treatment on the *c*-Si surface passivation quality, expressed by τ_{eff} (evaluated at $\Delta n=\Delta p=1.0\times10^{15}$ cm^{-3}), for doped *a*-Si:H stacks as shown in the inset sketches. Open symbols represent doped single films, closed symbols represent stacks, featuring an intrinsic buffer layer. Symmetric structures have been deposited on both wafer surfaces. Results for as deposited material are indicated in the abscissa by the label a.d. The data for the *a*-Si:H(p^+) films are taken from Ref. 34. Symbols represent experimental data; the lines are guides for the eye.

effective carrier-lifetime corrected for Auger-recombination, $\tau_{eff}^{-1}-\tau_{Auger}^{-1}$, as a function of the carrier-injection density, throughout the annealing experiment. All data can be fitted asymptotically to the expression of Kane and Swanson,[14]

$$\tau_{eff}^{-1}-\tau_{Auger}^{-1}=\tau_{SRH}^{-1}+2J_{0e}\frac{(N_D+\Delta n)}{qn_i^2W}, \quad (1)$$

where τ_{SRH} is the carrier lifetime limited by Shockley–Read–Hall (SRH) recombination in the wafer,[15,16] J_{0e} is the emitter saturation current, N_D and n_i are, respectively, the background doping and intrinsic carrier concentrations of the substrate and q is the elementary charge. W is the wafer thickness. This equation is valid for wafers featuring identical junctions at both surfaces. Here, it suggests that the surface passivation by the doped films is provided by a field effect rather than by chemical surface state passivation. Since high quality substrates were used, the SRH term may be neglected. Consequently, the fitting lines cut the abscissa at about $-N_D$. The figure shows that the slope of the curves (which is proportional to the value of J_{0e}) increases significantly with annealing (here with an activation energy, E_A, of about 0.7 eV). This may point at a reducing field effect, likely due to defect generation, counteracting the doping.

It is worth noting that at low injection the carrier lifetime increases remarkably, irrespective of the annealing conditions. This could point at carrier trapping,[17] which is known to occur in multicrystalline silicon,[18,19] but perhaps also at *c*-Si surfaces. This phenomenon is however absent in the *a*-Si:H(n^+)/*c*-Si(n) high-low junction case (not shown). Hence, more likely, the steady-state photoconductance of the *a*-Si:H(p^+)/*c*-Si(n) HJ is dominated by depletion-region modulation effects, at low injection.[20,21]

Figure 3 shows how the presence of a few nanometer thin intrinsic buffer layer underneath the doped films may affect the surface passivation quality throughout the annealing experiment. Note that for all films of similar dopant type, the deposition-times were exactly the same (see Table I). It is hence assumed that the superposed thickness of intrinsic and doped single-layers is equal to that of the corresponding doped/intrinsic stacked structure. The graph shows how for the *a*-Si:H(p^+) case the presence of an intrinsic buffer layer initially results in an improving passivation quality, although at about 220 °C degradation sets in. Underneath a *a*-Si:H(n^+) layer, the presence of a similar buffer layer film is even more benign. Here, the passivation quality improves throughout the full annealing cycle.

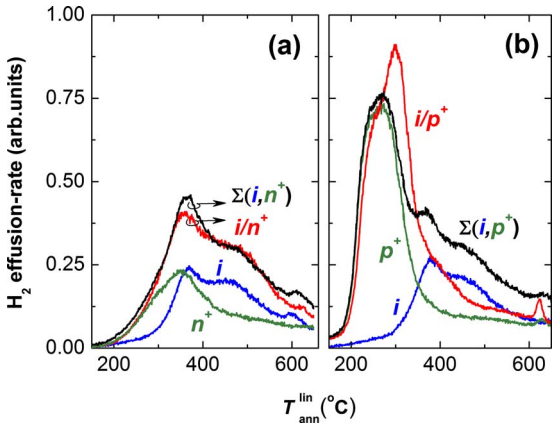

FIG. 4. (Color online) H_2 effusion data of the structures shown in Fig. 3. In each panel, the total thickness of the stacked layers is equal to the sum of the respective intrinsic and doped films. Panel (a) represents data for n^+-type, whereas in (b) the data are for p^+-type *a*-Si:H films. The latter data have been taken from Ref. 34.

Figure 4 shows H_2 effusion data for the samples displayed in Fig. 3. Panel (a) and (b), respectively, give data for n^+- and p^+-type *a*-Si:H structures. In addition, also the superposed signals of the single layers are displayed (label Σ). Doping of such thin *a*-Si:H films profoundly influences the H_2 effusion rate. Figure 4(b) shows that, compared to thin intrinsic *a*-Si:H films, for p^+ films, H_2 effusion occurs at significantly lower temperatures. Moreover, relatively more H_2 effuses at lower temperatures from a *a*-Si:H(p^+)/*a*-Si:H(i) stack than for the superposed films measured separately. Figure 4(a) gives TDS data for the *a*-Si:H(n^+) case. Also here, n^+-type doping results in H_2 effusing at lower temperatures, although the effect is not as drastic as for the p^+-type case. The data for the superposed intrinsic and n^+-type films (measured separately) seem now to match well to that of the *a*-Si:H(n^+)/*a*-Si:H(i) stack, within experimental error.

IV. DISCUSSION

A. Intrinsic *a*-Si:H film passivation

For an atomically sharp *a*-Si:H(i)/*c*-Si interface, low-temperature annealing improves the electronic interface passivation.[22] This is confirmed in Fig. 1 for films of only a few nanometer thick. Isothermal annealing of *a*-Si:H(i)/*c*-Si structures has been observed to yield stretched-exponential recombination decay.[23] For bulk *a*-Si:H material, defect reduction following similar functionals was explained in the

past as arising either from dispersive (i.e., time dependent) hydrogen diffusion[24] or from retrapping included hydrogen motion.[25] For the *a*-Si:H(*i*)/*c*-Si interface, based on the latter interpretation, the passivation improvement has been attributed to a transfer of hydrogen from a higher hydride state in the *a*-Si:H film (known to be dominant close to the interface),[26] to a monohydride *c*-Si surface state.[23,27] Consequently, the *a*-Si:H(*i*)/*c*-Si interface passivation is likely due to chemical surface state passivation, rather than due to a field effect.[23] It is worth noting that for a few nanometer thin *a*-Si:H(*i*) films, typically higher dangling bond densities are measured, compared to their thicker counterparts.[28] This may explain why also here the *a*-Si:H(*i*)/*c*-Si passivation quality is slightly inferior compared to previously obtained results with thicker (50 nm) films, deposited under similar conditions.[22]

B. Doped *a*-Si:H film passivation

For thin film *p-i-n* *a*-Si:H solar cells, the *p*-layer often has been argued to limit device performance. On the one hand, exposure of surfaces simultaneously to B_2H_6 and SiH_4 (before or after PECVD) may give rise to CVD growth of highly defective *a*-SiB_x:H layers, even at very low temperatures, resulting in poor *p-i* interfaces.[29,30] On the other hand, recombination in the *a*-Si:H(p^+) bulk itself was already for the first *p-i-n* devices recognized to hamper device performance.[31] Likely, this originates from doping induced localized states in the film.[32]

Here, as E_G^{opt} is mainly affected by the bonded H content (independent from the doping of the film),[33] its degradation under annealing [see Fig. 1(b)] suggests doping dependent Si–H rupture. The created defects may counteract the film doping and reduce thus the field effect (and interface passivation, see Fig. 2). The link between doping dependent Si–H rupture in the film and *a*-Si:H(p^+)/*c*-Si interface recombination was recently established based on H_2 effusion experiments as well.[34]

The effect of n^+-type doping appears to be less detrimental on the passivation properties, compared to that of p^+-type doping. Nevertheless, the study of equally thin phosphorous-doped *a*-Si:H(n^+) films by near-UV photoelectron constant final state yield spectroscopy (CFSYS)[35,36] has led to even more direct proof that also for a few nanometer thin films increased doping leads to increasing defect densities.[7] For n^+-type doping, these defects hinder the displacement of E_F toward the conduction band minimum (CBM), where also here such increased defect densities have been linked to enhanced recombination at the *a*-Si:H/*c*-Si interface.[7]

H_2 effusing at lower temperatures from doped (compared to undoped or compensated) *a*-Si:H films has been seen in the past as a proof that Si–H bond rupture (and thus defect generation) in such films depends on the position of E_F rather than on the physical nature of the present dopants.[37,38] This argument was originally used to explain doping dependent hydrogen diffusion phenomena in *a*-Si:H films.[39] The hydrogen diffusion energy E_D^*, defined by $D_H = D_0^* \exp(-E_D^*/kT)$, in *a*-Si:H and microcrystalline silicon (μc-Si) is displayed as function of E_F in Fig. 5. The data are

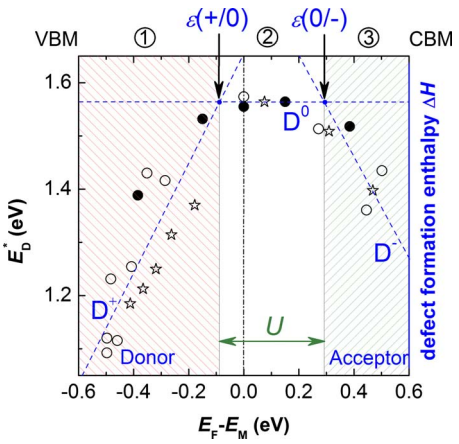

FIG. 5. (Color online) H diffusion energy E_D^* in *a*-Si:H (stars), μc-Si:H (open circles) or *c*-Si:H (closed circles) as a function of E_F, at T_{ann} = 350 °C. All data have been taken from Ref. 40. The *ad hoc* superposed straight lines represent the dependence of the formation enthalpy ΔH of defect D^q in the respective charge states q=+, 0, and −, on E_F (adapted after Ref. 45).

taken from Ref. 40. The diffusion coefficient, D_H, describes the motion of hydrogen in the silicon matrix, where $D_0^* = 10^{-3}$ cm^2 s^{-1} is the theoretical diffusion coefficient unaffected by traps,[41] k is the Boltzmann constant, and T is the temperature. The diffusion activation energy E_D^* equals E_S-μ_H, where E_S is the saddle point for interstitial H migration and μ_H is the chemical potential of H atoms.[42,43] The shown data imply that when E_F is closer to the valence band maximum (VBM) (i.e., *p*-type doping) this rapidly results in decreasing values for E_D^* (see crosshatched region with label ①). For *n*-type doping, E_F should be brought relatively closer to the CBM to yield a similar drop (crosshatched region with label ③).

The data in Fig. 4 confirm H_2 effusion occurring at higher temperatures for *n*- than for *p*-type *a*-Si:H films. This phenomenon is reflected in the passivation results as well (see Fig. 1). It is only at higher annealing temperatures that losses start to occur for *n*-type films, compared to their *p*-type counterparts. These trends suggest that *a*-Si:H/*c*-Si interface recombination may be related to E_F dependent Si–H rupture in the film, irrespective whether this film is *n*- or *p*-type.

Fundamentally, as the bandgap of a semiconductor increases, it often becomes increasingly difficult to dope it in a symmetric way (both *n*- and *p*-type). On the one hand, unintentional conductivity may originate from the presence of extrinsic impurities, such as, e.g., is the case for H in ZnO.[44] Native defects, on the other hand, can act as compensating centers that counteract intentional doping. Their formation depends on the position of E_F, according to the relation,[45]

$$\Delta H(D^q) = qE_F + n_D(\mu_D - \mu_{SH}) + \Delta E_b. \quad (2)$$

This relation describes the formation enthalpy of dopant D^q of charge state q (where q=−1, 0, or +1) in the semiconducting host. Here, μ_D and μ_{SH} are the chemical potentials of the dopants and host, n_D is the number of dopants, ΔE_b = E(host+defect)−E(host), and E is the total energy. The first term accounts for the fact that D^+ donates an electron, and

D^- accepts one. The transition level $\varepsilon(q+1/q)$ between charge states $q+1$ and q is defined as the position of E_F for which the formation energies of these charge states are equal.[46] Deliberate p-type (n-type) doping of the material by acceptors (donors) will shift E_F toward the VBM (CBM) and decrease the formation energy of native donors (acceptors) to a point where they are created spontaneously. Often, E_F cannot be brought beyond a certain point, the so-called the n- or p-type pinning energy $E_F^{(n \text{ or } p)}$, due to the occurring electronic compensation.[45]

In a-Si:H, it may be speculated that the described (asymmetric) E_F dependent defect generation is related to its relatively wide bandgap as well. Relation (2) can be sketched in Fig. 5 by the *ad hoc* superposed straight lines, approximately following the same trends as the experimental data. Here, the most likely formed defect by either type of doping is the amphoteric Si dangling bond D_3, backbonded to three Si atoms, via Si–H rupture.[47] At equilibrium, according to the position of E_F, this defect is either neutral (D_3^0), positively (D_3^+), or negatively (D_3^-) charged, accommodating, respectively, 1, 0, and 2 electrons, forming the foundations of the a-Si:H defect-pool model.[48,49] From the $+/0$ and $0/-$ transition levels, a correlation energy $U=\varepsilon(0/-)-\varepsilon(+/0)\approx +0.38$ eV is found, agreeing with values known for D_3 in a-Si:H.[50] This energy originates from Coulomb repulsion, possibly lowered by lattice relaxation at the defect-site.[51] Note that it is thanks to D_3's positive-U that a-Si:H can be intentionally doped relatively well; negative-U defects pin E_F.[51] Nevertheless, when E_F is located either in the [VBM, $\varepsilon(+/0)$] or [$\varepsilon(0/-)$, CBM] area of the bandgap (both of which are crosshatched in Fig. 5, respectively, with labels ① and ③), D_3 will behave as a compensating center, counteracting the intentional doping. In these cases, the formation energy of a dangling bond, compared to its neutral state, is reduced by an amount, respectively, equal to $\Delta E^+(E_F)=[\varepsilon(+/0)-E_F]$ and $\Delta E^-(E_F)=[E_F-\varepsilon(0/-)]$.[52,53] The diffusion activation energy E_D^* is reduced by similar amounts. These arguments lead to conclude that the doping asymmetry of a-Si:H films (and thus, as argued, their difference in c-Si surface passivation quality) originates from the asymmetrical location of the D_3^+ and D_3^- states in the a-Si:H bandgap.

To increase the thermal stability (and thus doping efficiency) of p-type (n-type) material, it has been argued that the VBM (CBM) should be closer to (further away from) the vacuum level.[45] Fullfilling both conditions yields a reduced bandgap material. For a-Si:H films, this can be accomplished by optimizing deposition conditions toward a lowered bonded hydrogen content of the films,[33] corresponding to denser material.[54,55] This argument may explain why the surface passivation properties of μc-Si(p^+) films [deposited on a-Si:H(i) buffer layers] appear to be superior, compared to their wider bandgap a-Si:H(p^+) counterparts.[56,57] Moreover, the use of μc-Si(p^+) films may also resolve possible contact problems between transparent conductive oxide and the p-type film, during device fabrication.[57,58] Care has to be taken to deposit such denser material for the intrinsic buffer layer, however, as it will easily result in undesired epitaxial growth.

C. Stacked film passivation: Intrinsic buffer layer

For structures that feature a thin intrinsic buffer layer, initially the passivation improves for both the a-Si:H(p^+)/a-Si:H(i)/c-Si and the a-Si:H(n^+)/a-Si:H(i)/c-Si case (Fig. 3). Likely, this originates again from hydrogenation of c-Si surface states at the a-Si:H(i)/c-Si interface, as described before. Nevertheless, for the a-Si:H(p^+)/a-Si:H(i)/c-Si case, from annealing at about 220 °C onwards, degradation sets in. For c-Si(n) HJ solar cells featuring such a a-Si:H(p^+) emitter, postdeposition annealing at moderate temperatures has been observed to result in a similar local optimum for the value of the open circuit voltage, V_{oc}.[59] It has been argued that the loss in passivation is caused by Si–H rupture in the intrinsic buffer layer, occurring at lower temperatures for the stacked a-Si:H(p^+)/a-Si:H(i)/c-Si structure compared to the a-Si:H(i)/c-Si case (lacking the a-Si:H(p^+) overlayer).[34] This is evidenced in Fig. 4, where for the stacked a-Si:H(p^+)/a-Si:H(i)/c-Si structure more H_2 effuses out at low temperatures, compared to the superposed a-Si:H(p^+)/c-Si and a-Si:H(i)/c-Si structures (label Σ in the figure). This phenomenon was also observed by Einsele *et al.* (Ref. 60), and can be explained by Fig. 5: Due to the presence of the p^+-type overlayer, an electrical field will now be present in the intrinsic buffer layer, pulling also here E_F closer to the VBM, likely into the [VBM, $\varepsilon(+/0)$] area (with label ①), and thus lowering the defect formation energy.

For the a-Si:H(n^+)/a-Si:H(i)/c-Si case, the passivation trend has the same tendency as the same structure lacking the a-Si:H(n^+) overlayer: No degradation is observed. This result agrees well with the H_2 effusion data presented in panel a of Fig. 4. Here, the signals for the stacked a-Si:H(n^+)/a-Si:H(i)/c-Si case are (within experimental error) equal to the superposed a-Si:H(i)/c-Si and a-Si:H(n^+)/c-Si cases (label Σ in the figure). Consequently, in contrast to the p^+-type case, an n^+-type overlayer does not lower the Si–H bond rupture energy in the underlying intrinsic film. This is consistent again with Fig. 5. Also here it must be assumed that E_F is shifted closer to the CBM in the buffer layer. Most likely, however, this shift is not sufficiently large to bring E_F into the [$\varepsilon(0/-)$, CBM] region (label ③). The fact that the passivation quality of the a-Si:H(n^+)/a-Si:H(i)/c-Si structure is slightly superior to that of the a-Si:H(i)/c-Si case could now perhaps be explained by an additional field effect, repelling holes from the c-Si surface states, but unsufficiently strong to reduce the chemical a-Si:H/c-Si interface passivation.

V. CONCLUSIONS

In this article, it has been argued that doped a-Si:H/c-Si interface recombination may result from Fermi energy dependent defect generation in the passivating layer, counteracting the intentional doping. For a-Si:H films, for both types of doping, this defect is likely the amphoteric Si dangling bond, created by Si–H rupture, as evidenced from H_2 effusion and spectroscopic ellipsometry data. Interface passivation losses that may occur in case an intrinsic buffer layer is present (underneath the doped layers) could be ex-

plained consistently according to the same thermodynamic model. Further work is needed to obtain more quantitative proof of these assumptions, by methods such as, e.g., photoelectron CFSYS on these thin *a*-Si:H films.

ACKNOWLEDGMENTS

This work was supported, respectively, by the New Energy and Industrial Technology Development Organization (NEDO), Japan, by the European Community's Seventh Framework Programme [FP/2007–2013] under the Hetsi Project (Grant Agreement No. 211821), and by Axpo Holding AG, Switzerland, in the frame of the Axpo Naturstrom Fonds.

[1]E. Yablonovitch, T. Gmitter, R. M. Swanson, and Y. H. Kwark, Appl. Phys. Lett. **47**, 1211 (1986).
[2]J. I. Pankove and M. L. Tarng, Appl. Phys. Lett. **34**, 156 (1979).
[3]H. Matsuura, T. Okuno, H. Okushi, and K. Tanaka, J. Appl. Phys. **55**, 1012 (1984).
[4]J. G. Fossum, IEEE Trans. Electron Devices **24**, 322 (1977).
[5]M. Taguchi, A. Terakawa, E. Maruyama, and M. Tanaka, Prog. Photovoltaics **13**, 481 (2005).
[6]S. De Wolf and G. Beaucarne, Appl. Phys. Lett. **88**, 022104 (2006).
[7]L. Korte and M. Schmidt, J. Non-Cryst. Solids **354**, 2138 (2008).
[8]M. Tanaka, M. Taguchi, T. Matsuyama, T. Sawada, S. Tsuda, S. Nakano, H. Hanafusa, and Y. Kuwano, Jpn. J. Appl. Phys., Part 1 **31**, 3518 (1992).
[9]Y. Tsunomura, Y. Yoshimine, M. Taguchi, T. Baba, T. Kinoshita, H. Kanno, H. Sakata, E. Maruyama, and M. Tanaka, Sol. Energy Mater. Sol. Cells **93**, 670 (2008).
[10]M. A. Green, K. Emery, Y. Hishikawa, and W. Warta, Prog. Photovoltaics **16**, 435 (2008).
[11]S. De Wolf, G. Agostinelli, G. Beaucarne, and P. Vitanov, J. Appl. Phys. **97**, 063303 (2005).
[12]R. A. Sinton and A. Cuevas, Appl. Phys. Lett. **69**, 2510 (1996).
[13]H. Fujiwara, *Spectroscopic Ellipsometry: Principles and Applications* (Wiley, Chichester, England, 2007).
[14]D. E. Kane and R. M. Swanson, Proceedings of the 16th IEEE Photovoltaic Specialists Conference, Las Vegas, Nevada (IEEE, Piscataway, NJ, 1985), p. 578.
[15]W. Shockley and W. T. Read, Phys. Rev. **57**, 835 (1952).
[16]R. N. Hall, Phys. Rev. **57**, 387 (1952).
[17]J. A. Hornbeck and J. R. Haynes, Phys. Rev. **97**, 311 (1955).
[18]D. Macdonald and A. Cuevas, Appl. Phys. Lett. **74**, 1710 (1999).
[19]H. F. W. Dekkers, L. Carnel, and G. Beaucarne, Appl. Phys. Lett. **89**, 013508 (2006).
[20]M. Bail, M. Schulz, and R. Brendel, Appl. Phys. Lett. **82**, 757 (2003).
[21]P. J. Cousins, D. H. Neuhaus, and J. E. Cotter, J. Appl. Phys. **95**, 1854 (2004).
[22]S. De Wolf and M. Kondo, Appl. Phys. Lett. **90**, 042111 (2007).
[23]S. De Wolf, S. Olibet, and C. Ballif, Appl. Phys. Lett. **93**, 032101 (2008).
[24]J. Kakalios, R. A. Street, and W. B. Jackson, Phys. Rev. Lett. **59**, 1037 (1987).
[25]C. G. Van de Walle, Phys. Rev. B **53**, 11292 (1996).
[26]H. Fujiwara and M. Kondo, Appl. Phys. Lett. **86**, 032112 (2005).
[27]M. Z. Burrows, U. K. Das, R. L. Opila, S. De Wolf, and R. W. Birkmire, J. Vac. Sci. Technol. A **26**, 683 (2008).
[28]L. Korte, A. Laades, and M. Schmidt, J. Non-Cryst. Solids **352**, 1217 (2006).
[29]A. Catalano and G. Wood, J. Appl. Phys. **63**, 1220 (1988).
[30]R. W. Collins, Appl. Phys. Lett. **53**, 1086 (1988).
[31]D. E. Carlson and C. R. Wronski, Appl. Phys. Lett. **28**, 671 (1976).
[32]R.A. Street, J. Non-Cryst. Solids **77–78**, 1 (1985).
[33]A. Matsuda, M. Matsumura, S. Yamasaki, H. Yamamoto, T. Imura, H. Okushi, S. Izima, and K. Tanaka, Jpn. J. Appl. Phys. **20**, L183 (1981).
[34]S. De Wolf and M. Kondo, Appl. Phys. Lett. **91**, 112109 (2007).
[35]M. Sebastiani, L. Di Gaspare, G. Capellini, C. Bittencourt, and F. Evangelisti, Phys. Rev. Lett. **75**, 3352 (1995).
[36]M. Schmidt, A. Schoepke, L. Korte, O. Milch, and W. Fuhs, J. Non-Cryst. Solids **338**, 211 (2004).
[37]W. Beyer, J. Herion, and H. Wagner, J. Non-Cryst. Solids **114**, 217 (1989).
[38]W. Beyer, Physica B **170**, 105 (1991).
[39]R. A. Street, C. C. Tsai, J. Kakalios, and W. B. Jackson, Philos. Mag. B **56**, 305 (1987).
[40]W. Beyer and U. Zastrow, Mater. Res. Soc. Symp. Proc. **609**, A20.4 (2000).
[41]W. Beyer, *Semiconductors and Semimetals* (Academic, San Diego, 1999), Vol. 61, p. 165.
[42]R. A. Street, Physica B **170**, 69 (1991).
[43]C. G. Van de Walle and R. A. Street, Phys. Rev. B **51**, 10615 (1995).
[44]C. G. Van de Walle, Phys. Rev. Lett. **85**, 1012 (2000).
[45]A. Zunger, Appl. Phys. Lett. **83**, 57 (2003).
[46]C. G. Van de Walle, Phys. Status Solidi B **229**, 221 (2002).
[47]R. A. Street, D. K. Biegelsen, and J. C. Knights, Phys. Rev. B **24**, 969 (1981).
[48]K. Winer, Phys. Rev. Lett. **63**, 1487 (1989).
[49]M. J. Powell and S. C. Deane, Phys. Rev. B **48**, 10815 (1994).
[50]W. B. Jackson, Solid State Commun. **44**, 477 (1982).
[51]R. A. Street, *Hydrogenated Amorphous Silicon* (Cambridge University, Cambridge, 1991).
[52]Y. Bar-Yam, D. Adler, and J. D. Joannopoulos, Phys. Rev. Lett. **57**, 467 (1986).
[53]H. M. Branz, Phys. Rev. B **39**, 5107 (1989).
[54]H. Fritzsche, M. Tanielian, C. C. Tsai, and P. J. Gaczi, J. Appl. Phys. **50**, 3366 (1979).
[55]A. H. M. Smets, W. M. M. Kessels, and M. C. M. van de Sanden, Appl. Phys. Lett. **82**, 1547 (2003).
[56]P. J. Rostan, U. Rau, V. X. Nguyen, T. Kirchartz, M. B. Schubert, and J. H. Werner, Sol. Energy Mater. Sol. Cells **90**, 1345 (2006).
[57]F. Einsele, P. J. Rostan, M. B. Schubert, and U. Rau, J. Appl. Phys. **102**, 094507 (2007).
[58]H. Stiebig, F. Siebke, W. Beyer, C. Beneking, B. Rech, and H. Wagner, Sol. Energy Mater. Sol. Cells **48**, 351 (1997).
[59]T. Koida, H. Fujiwara, and M. Kondo, Appl. Phys. Express **1**, 04501 (2008).
[60]F. Einsele, W. Beyer, and U. Rau, Proceedings of the 23rd European Photovoltaic Solar Energy Conference and Exhibition, Valencia, Spain (WIP, Munich, 2008).